Phillips, M. C., & Hauser, H. (1974) *J. Colloid Interface Sci. 49*, 31.
Pons, M., Johnston, D. S., & Chapman, D. (1982) *J. Polym. Sci., Polym. Lett. Ed. 20*, 513.
Stoeckenius, W. (1962) *J. Cell Biol. 12*, 221.
Stoffel, W., Salm, K.-P., & Muller, U. (1982) *Hoppe-Seyler's Z. Physiol. Chem. 363*, 1.
Tieke, B., & Bloor, D. (1979) *Makromol. Chem. 180*, 2275.

Resonance Raman Spectra of Copper(II)-Substituted Liver Alcohol Dehydrogenase: A Type 1 Copper Analogue†

Wolfgang Maret, Michael Zeppezauer, Joann Sanders-Loehr, and Thomas M. Loehr*

ABSTRACT: Liver alcohol dehydrogenase (LADH) with copper in place of the catalytic zinc has recently been proposed to contain a type 1 site analogous to that in "blue" copper proteins. Resonance Raman spectra for the copper-substituted enzyme, Cu(II)·LADH, and its binary complexes with reduced nicotinamide adenine dinucleotide (NADH) and pyrazole support this viewpoint. These spectra have two dominant features: a sharp peak at ~415 cm^{-1}, which is believed to be associated with vibration of the single histidine ligand, and a broader, asymmetric band at ~350 cm^{-1}, whose components are assigned predominantly to vibrational modes of the two cysteinate ligands. The high frequency of these transitions, which is reminiscent of the blue copper proteins, is ascribed to the tetrahedral nature of the metal site that produces unusually short Cu–S bonds and coupled vibrational modes. Solvent exchange with $H_2{}^{18}O$ reveals no contribution to the resonance Raman spectrum of the water molecule, which is a metal ligand in free Cu(II)·LADH; however, the spectrum of the binary complex with pyrazole has several new peaks attributable, in part, to pyrazole ligation. The strong similarity among the vibrational spectra demonstrates that the Cu(II) environment in alcohol dehydrogenase maintains its near-tetrahedral geometry in the various enzyme derivatives. The resonance Raman spectrum of Ni(II)·LADH is close to that of Cu(II)·LADH and suggests a similar tetrahedral site. The Raman spectra presented here together with available optical and EPR data indicate that Cu(II)·LADH belongs to the type 1 copper classification and, thus, can provide new insights into this unusual coordination geometry.

Alcohol dehydrogenase from horse liver is a dimeric molecule wherein each subunit contains two zinc ions. The metal-site structures of these ions are known from X-ray crystallography and include a structural zinc that is coordinated to four cysteinates and a catalytic zinc that is coordinated to two cysteinates, one histidine, and one water molecule (Eklund et al., 1976). Recently, Maret and co-workers (Maret et al., 1980) prepared a derivative of liver alcohol dehydrogenase (LADH)[1] in which the catalytic zinc was substituted by copper. Characterization of this cupric protein by optical and EPR measurements (Maret et al., 1980, 1981) showed Cu(II)·LADH to be strikingly similar to the "blue" copper proteins such as azurin, plastocyanin, and stellacyanin and the type 1 sites of several multicopper oxidases such as laccase and ascorbate oxidase (Fee, 1975). The optical absorption spectrum of Cu(II)·LADH at 296 K has an intense band at 620 nm ($\epsilon \simeq 4000$ M^{-1} cm^{-1}), and the EPR spectrum at 100 K exhibits rhombic character with $g_\parallel = 2.21$ and $A_\parallel = 0.005$ cm^{-1} (Maret et al., 1983).[2] The anomalously small hyperfine coupling constant and the intense electronic absorption of the type 1 site have been explained as arising from thiolate coordination of Cu(II) in a distorted tetrahedral environment with the characteristic absorption at ≃600 nm being assigned to cysteinate sulfur → Cu(II) charge transfer (Gray & Solomon, 1981). Thus, it is of interest to learn whether similar structural parameters are present in Cu(II)·LADH.

Resonance Raman spectroscopy appears to be a valuable technique for probing the structure and bonding of the type 1 site chromophore. All of the blue copper proteins that have been investigated show the following common features in their resonance Raman spectra: (i) three or more strong bands between 350 and 450 cm^{-1} that are associated with vibrations of the copper chromophore; (ii) intensity enhancement of these vibrations via resonance with the ≃600-nm LMCT band; and (iii) two nearly constant frequency vibrational modes at ≃750 and ≃260 cm^{-1} (Miskowski et al., 1975; Siiman et al., 1976; Ferris et al., 1979). The unexpectedly high frequencies of the Cu(II)–ligand vibrations (when compared with inorganic Cu(II) complexes) can be explained by the shortness of the Cu–S(Cys) bond and the tetrahedral character of the copper binding site that have been observed in the crystal structure of plastocyanin (Freeman, 1981). A normal coordinate

† From the Universität des Saarlandes, Analytische und Biologische Chemie, Fachbereich 15.2, D-6600 Saarbrücken 11, FRG (W.M. and M.Z.), the Department of Chemistry, Portland State University, Portland, Oregon 97207 (J.S.-L.), and the Department of Chemistry and Biochemical Sciences, Oregon Graduate Center, Beaverton, Oregon 97006 (T.M.L.). *Received January 31, 1983.* This work was supported by the U.S. Public Health Service, National Institutes of Health (GM18865).

[1] Abbreviations: LADH, liver alcohol dehydrogenase; EPR, electron paramagnetic resonance; NADH, reduced nicotinamide adenine dinucleotide; Tes, 2-[[tris(hydroxymethyl)methyl]amino]-1-ethanesulfonic acid; LMCT, ligand to metal charge transfer; ^1H NMR, proton nuclear magnetic resonance. Metal ion derivatives of LADH, M(II)·LADH, used throughout this paper refer to metal substitution solely in the catalytic site.

[2] Maret et al. (1980) initially reported values for $g_\parallel$ and $A_\parallel$ of 2.25 and 0.003 cm^{-1}, respectively, from an enzyme preparation having ≃60% site-specific replacement of Cu(II); the present values are a redetermination for Cu(II)·LADH of significantly higher copper content in the active site (≃80%).

0006-2960/83/0422-3202$01.50/0

analysis of the type 1 copper site of azurin indicates that the multiplicity of bands in the 350–450-cm^{-1} region is due to strong coupling of the Cu–S(cysteinate) and Cu–imidazole vibrational modes, that the frequencies are sensitive to the coordination geometry of the Cu(II) chromophore, and that a three- or four-coordinate copper ion in a tetrahedral environment gives the best fit with the observed resonance Raman spectrum (Thamann et al., 1982).

In native liver alcohol dehydrogenase, the active site zinc ion has a tetrahedral coordination geometry (Eklund et al., 1976). Since metal-substituted species such as Ni(II)·LADH and Co(II)·LADH exhibit similar enzymatic properties to those of Zn(II)·LADH (Dunn et al., 1982), the metal ions are likely to be present in similar coordination environments. An X-ray crystallographic investigation of Co(II)·LADH has shown that the cobalt ion is bound in the same coordination geometry as the zinc ion in Zn(II)·LADH (Schneider et al., 1983). The structure of the copper-substituted protein is less certain due to its poor enzymatic activity. However, the presence of a metal-bound water molecule, as in the native enzyme, has been demonstrated for Cu(II)·LADH by magnetic relaxation studies (Andersson et al., 1981). The Raman spectra reported here provide evidence, by analogy to blue copper proteins of known structure, that the copper in LADH is also coordinated to two cysteines and one histidine in a tetrahedral environment.

Experimental Procedures

Horse liver alcohol dehydrogenase (EC 1.1.1.1) and NADH (grade I) were obtained from Boehringer-Mannheim. All chemicals were analytical grade. Oxygen-18-enriched water (90.43 atom % ^{18}O, Monsanto Co.) was the generous gift of Dr. M. W. Makinen. The removal of Zn(II) and reconstitution with Cu(II) and Ni(II) specific for the catalytic site were carried out as described previously (Maret et al., 1980; Dietrich et al., 1981). The crystalline metalloenzymes were dissolved in 25 mM Tes at pH 7 with the addition of solid NaCl to a final concentration of 0.3–0.5 M chloride in order to obtain concentrated protein samples. This concentration of chloride does not appear to have any effects upon the metal center of either the zinc or the copper enzyme. The metal content of the copper enzyme was measured by atomic absorption spectroscopy and found to correspond to 1.6 mol of copper/dimer. The extinction coefficient at 620 nm was determined to be ~4000 M^{-1} cm^{-1}. The nickel content was calculated from the known extinction coefficient of Ni(II)·LADH and was 1.4 mol of nickel/dimer. Addition of ligands was carried out under a nitrogen atmosphere.

Protein samples for the Raman experiments were loaded into nitrogen-flushed glass melting-point capillaries and filled by syringe under a cover of nitrogen gas. The capillaries were held in a cold-finger Dewar (Sjöberg et al., 1982). Raman data were collected on a computer-interfaced Jarrell-Ash spectrophotometer (Loehr et al., 1979) equipped with Spectra-Physics Model 164 Ar and Kr lasers, an ITT FW-130 photomultiplier tube (S-20 photocathode at ~245 K), and an Ortec Model 9302 amplifier–discriminator. Most of the spectra were improved in signal to noise by repetitive scanning by the automated data collection procedure. Peak positions of sharp peaks are accurate to ±1 cm^{-1} whereas weak or broad peaks are judged to be accurate to ±2 cm^{-1}. Resonance Raman spectra of Cu(II)·LADH obtained with 568.2-nm excitation were indistinguishable from those obtained with 647.1-nm excitation. Data from solution samples at ≃275 K were also qualitatively identical with data from frozen solutions at ≃77 K. However, somewhat better spectral resolution and enhanced signal to noise were obtained at low temperature.

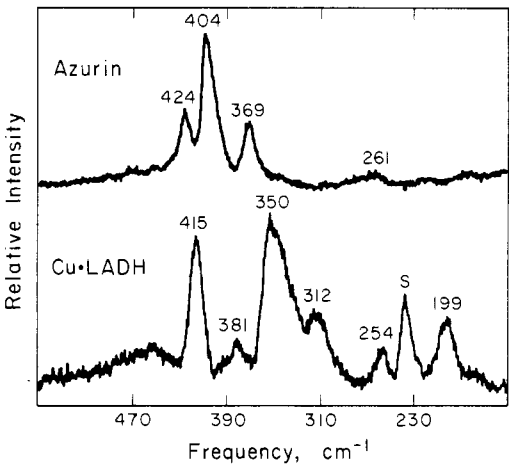

FIGURE 1: Resonance Raman spectra of azurin from *Pseudomonas aeruginosa* and Cu(II)-substituted alcohol dehydrogenase using 647.1-nm excitation. Conditions for azurin: ~1 mM protein in 50 mM ammonium acetate, pH 6.0 at ~275 K; sum of 67 scans; see Thamann et al. (1982) for further spectral details. Conditions for Cu(II)·LADH: 2.3 mM protein in 25 mM Tes–0.5 M NaCl, pH 7.0 at ~77 K; sum of eight scans. General conditions for LADH samples: 2 cm^{-1}/s scan rate, 10-cm^{-1} slit width, ~100-mW laser power at the sample Dewar. S denotes a spectral contribution from frozen solvent.

Results and Discussion

Azurin and Blue Copper Proteins. The resonance Raman spectrum of azurin, as a representative blue copper protein, is shown in Figure 1. This spectrum has three dominant peaks at 424, 404 and 369 cm^{-1}. The appearance of three or more intense bands in this narrow 350–450-cm^{-1} frequency range, several weaker spectral features between 100 and 550 cm^{-1}, and a series of bands between 700 and 850 cm^{-1} are spectral properties common to all the blue copper proteins. We have assigned the 369-cm^{-1} band of the azurin spectrum to predominantly Cu–S(Cys) stretching and the two >400-cm^{-1} bands to predominantly Cu–N(imidazole) modes, with the qualification that all of these vibrational motions appear to be highly coupled in these tetrahedral chromophores (Thamann et al., 1982). The appearance of the several weaker spectral bands suggests that metal–ligand and/or ligand deformation modes are also resonance enhanced. For example, we have assigned the band at ~260 cm^{-1} that seems to be present in the spectra of all of the blue copper proteins to a Cu–S–C deformation of the cysteinate ligand. Moreover, the nearly constant ~750-cm^{-1} band occurs at a plausible frequency for the C–S vibration of this common ligand (Thamann et al., 1982). Other bands above 700 cm^{-1} are well accounted for as overtones and combinations of the signature bands in the 350–450-cm^{-1} domain (Ferris et al., 1979).

Cu(II)·LADH. The resonance Raman spectrum of Cu(II)·LADH is also shown in Figure 1. There are two intense peaks at 415 and 350 cm^{-1}, with the asymmetry of the latter being indicative of at least two components. There are also a number of lower intensity bands including a distinct feature at 254 cm^{-1} and a moderately intense peak at 750 cm^{-1} (not shown). This 750-cm^{-1} band is accompanied by a shoulder at ~765 cm^{-1} and another distinct peak at ~697 cm^{-1}. Qualitatively, then, the Cu(II)·LADH resonance Raman spectrum is quite similar to the general spectral pattern of the blue copper proteins, indicating that the structure of the copper ion site in LADH must also have a near-tetrahedral geometry and unusually short Cu–S bonds. The corresponding Cu–S(cysteinate) bond length has been determined to be ≃2.10 Å

Table I: Electronic, EPR, and Resonance Raman Spectral Data for Copper- and Nickel-Substituted Alcohol Dehydrogenase[a]

enzyme	λ_{max} (nm) 296 K	λ_{max} (nm) 77 K	$A_{\parallel}$ ($\times 10^4$ cm^{-1}) at 100 K	vibrational frequencies (cm^{-1}) at 77 K[b] ν_a	ν_b	ν_c	ν_d
Cu(II)·LADH	620	580	50[c]	415	350	254	199
+NADH		680	<30	420	359	263	202
+pyrazole	620	495	115	413	368	246	196
Ni(II)·LADH[d]	407			413	350	255	

[a] Electronic and EPR data from Maret et al. (1980, 1981); the λ_{max} is the position of the S_{σ}(Cys) → M(II)·LMCT. [b] Selected prominent and characteristic frequencies; ν_a, ν_b, and ν_c are assigned in the text; ν_d is unassigned. [c] W. Maret, M. Zeppezauer, A. Desideri, L. Morpurgo, and G. Rotilio, unpublished results. [d] Raman data obtained with 406.7-nm excitation on a 1.8 mM sample in 25 mM Tes–0.5 M NaCl, pH 7.

in both azurin (Tullius et al., 1978) and plastocyanin (Freeman, 1981; Scott et al., 1982).

The appearance of a single, distinct peak at 415 cm^{-1} with a broad and asymmetric band at ≃350 cm^{-1} in the resonance Raman spectrum of Cu(II)·LADH is consistent with the vibrational assignments proposed for azurin. The 415-cm^{-1} peak would arise primarily from the contribution of *one* histidine ligand (vs. *two* in azurin), whereas the composite 350-cm^{-1} band apparently reflects the presence of *two* cysteinates (vs. *one* in azurin). The peaks at 750 and 254 cm^{-1} in Cu(II)·LADH seem analogous to their counterparts in the blue copper proteins and are assignable to C–S stretching and Cu–S–C deformations, respectively, of ligated cysteines. The possible contributions of two cysteine ligands are also suggested by the higher intensity of the 254-cm^{-1} peak in Cu(II)·LADH relative to azurin. The additional features at ≃765 and ≃697 cm^{-1} are attributed to a combination mode (415 cm^{-1} + 350 cm^{-1} = 765 cm^{-1}) and an overtone (2 × 350 cm^{-1} = 700 cm^{-1}), respectively. The remaining peaks at 381, 312, and 199 cm^{-1} (Figure 1) appear to be more characteristic of Cu(II)·LADH than of the type 1 copper proteins, but no specific assignments can be made at this time.

When crystals of Cu(II)·LADH were dissolved to 3.9 mM in $H_2{}^{18}O$ with the addition of solid NaCl, an identical resonance Raman spectrum was observed compared to that shown in Figure 1. The only spectral feature sensitive to the isotopically enriched water was the ≃230-cm^{-1} solvent band (characteristic of ice and seen in all frozen samples) that shifted to ~220 cm^{-1} in $H_2{}^{18}O$. It seems clear that the water molecule present as the fourth ligand does not contribute to the resonance Raman spectrum obtained by excitation within the 620-nm absorption band. Since the observed spectrum is well described by the Cu(II)–cysteinate chromophore having coupled vibrations with imidazole modes of the ligated histidine (Thamann et al., 1982), this coupling apparently does not extend to the bound water molecule.

Binary Complex of Cu(II)·LADH with Coenzyme. The crystal structure of the native zinc enzyme shows that the coenzyme has a specific binding site close to the catalytic site with its nicotinamide ring within van der Waals contact of the catalytic metal ion (Eklund et al., 1981; Cedergren-Zeppezauer et al., 1982). The coenzyme induces a significant protein conformational change, enhancing the substrate binding in a more hydrophobic metal ion environment. Although coenzyme binding produces no change in zinc ligands (Eklund et al., 1981; Cedergren-Zeppezauer et al., 1982), it is possible that the changes in protein conformation do cause small perturbations at the metal center.

Cu(II) substitution for the spectroscopically silent Zn(II) has permitted the investigation of coenzyme binding by optical and EPR methods. The 296 K optical spectrum of Cu(II)·LADH shows a small red shift upon NADH binding (Table I), but the molar extinction remains unchanged (W. Maret, unpublished results). The hyperfine splitting of Cu(II)·LADH changes only slightly upon NADH binding (Table I). Taken together, the electronic spectral and EPR data suggest only minimal perturbation of the Cu(II) site upon binary complex formation with the coenzyme and retention of a type 1 classification.

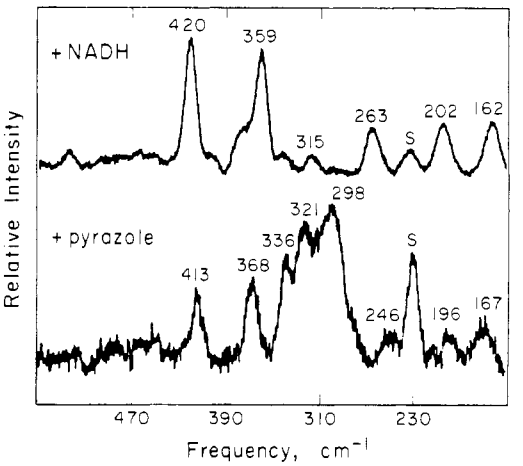

FIGURE 2: Resonance Raman spectra of binary complexes of Cu(II)-substituted alcohol dehydrogenase with cofactor NADH and pyrazole, respectively, obtained on frozen solutions at ~77 K. (Upper spectrum) 2.1 mM Cu·LADH and 123 mM NADH in 25 mM Tes–0.5 M NaCl, pH 7.0; sum of 57 scans using 647.1-nm excitation. (Lower spectrum) 2.1 mM Cu(II)·LADH and 123 mM pyrazole in 25 mM Tes–0.5 M NaCl, pH 7.0; sum of 12 scans using 496.5-nm laser light passed through a narrow band-pass interference filter. Similar results were obtained with 488.0- and 514.5-nm excitations. General conditions as in Figure 1.

The resonance Raman spectrum of the Cu(II)·LADH/NADH complex (Figure 2, upper spectrum) reveals a number of small changes relative to that of Cu(II)·LADH. The 415-cm^{-1} peak is slightly increased in energy, and the 350-cm^{-1} band is raised by ~9 cm^{-1} and now exhibits asymmetry on the high-frequency side. In addition, two new spectral contributions are seen at ~520 and 162 cm^{-1}, neither of which appears in a frozen solution spectrum of buffer plus NADH without Cu(II)·LADH. Despite a number of frequency shifts and the appearance of at least two new spectral features, the general pattern previously observed for Cu(II)·LADH (Figure 1) is preserved. We conclude that the Cu(II) coordination and site geometry are basically unaltered in the NADH complex. The differences that are observed in the resonance Raman spectrum of the binary complex of Cu(II)·LADH with the coenzyme may relate to small protein conformational differences being expressed at the metal site. For example, inequivalence of the two sulfur ligands is probable as revealed by the different contributions to the ≃350-cm^{-1} vibrational frequency in the two spectra.

Binary Complex of Cu(II)·LADH with Pyrazole. Pyrazole is a competitive inhibitor of alcohol oxidation in the native

enzyme. It binds directly to the metal ion in the binary complex Zn(II)·LADH/pyrazole and in the ternary complex Zn(II)·LADH/pyrazole/NAD^+ as has been shown crystallographically (Eklund et al., 1982). The Cu(II)-substituted alcohol dehydrogenase reacts with pyrazole, leading to reduction of copper in a few seconds at room temperature (Maret et al., 1980). Despite the fleeting existence of this complex, its ambient-temperature optical absorption still shows a λ_{max} at ~620 nm. However, the pyrazole adduct is stable to reduction at liquid-nitrogen temperatures, where its absorption maximum is blue shifted by over 4000 cm^{-1} to ~495 nm (Table I). The EPR spectrum of this low-temperature species has axial symmetry, and the hyperfine splitting, $A_\parallel$, has increased to 115×10^{-4} cm^{-1} (Table I). Moreover, pyrazole ligation to the Cu(II) site is evident from the presence of additional nitrogen superhyperfine structure in the $g_\perp$ region. These spectral changes have been interpreted as a possible change in geometry of the copper site, perhaps one closer to square planar, but without adopting a type 2 site classification in view of the remaining intense charge-transfer band at 495 nm at 77 K (Maret et al., 1980).

The resonance Raman spectrum of the binary complex Cu(II)·LADH/pyrazole obtained with 496.5-nm excitation is shown in Figure 2. This spectrum is notably different from the Cu(II)·LADH data shown in Figures 1 and 2 by the appearance of a series of three strong bands at 336, 321 and 298 cm^{-1}. It is noteworthy, however, that these new spectral features are superimposed upon a spectrum characteristic of Cu(II)·LADH. Thus, the resonance Raman spectrum of the pyrazole adduct again reveals two principal peaks (at 413 and 368 cm^{-1}), as well as lower intensity features at 246, 196 and 167 cm^{-1}. The 368-cm^{-1} peak is higher in energy than previously observed and appears to be symmetrical in shape. It is possible that the second component, previously noted as a shoulder to the ~350-cm^{-1} band, is now the distinct peak at 336 cm^{-1} and that only the 321- and 298-cm^{-1} features are due to the ligated pyrazole participating in resonance enhancement of the vibrational modes of the new chromophore. However, no firm assignments can be made in the absence of confirming isotopic-substitution experiments.

The retention of the characteristic Cu(II)·LADH resonance Raman spectrum in the pyrazole complex (Table I) strongly argues for maintenance of the copper site structure. In our normal coordinate analysis of a CuN_2S_2 structure, geometrical variations alone, while maintaining the bond lengths and the force field, did give rise to significant variability in calculated frequencies for skeletal modes (Thamann et al., 1982). Thus, a substantial distortion away from tetrahedral geometry would have been expected to generate a more markedly different Raman spectrum. If the shift in λ_{max} and increase in $A_\parallel$ in the Cu(II)·LADH/pyrazole complex are indeed due to a structural change, it must be a fairly subtle one. This is supported by the fact that the structurally sensitive EPR and optical changes are induced solely by a change in temperature. Thus, Cu(II)·LADH adducts appear to retain the Raman and EPR properties of the type 1 sites more faithfully than their optical properties (Table I).

Ni(II)·LADH. The preparation of the Ni(II) derivative of alcohol dehydrogenase was described by Dietrich et al. (1981). The dominant S_σ(Cys) → Ni(II) charge-transfer band at 24 600 cm^{-1} (407 nm) in Ni(II)·LADH and at 22 700 cm^{-1} (440 nm) in its pyrazole complex is considerably blue shifted relative to the copper derivative (Table I). Nonetheless, the position of this LMCT band still argues strongly for a tetrahedral site, since it lies some 12 000 cm^{-1} toward *lower* energy than would be expected for a square-planar Ni(II). As an example, a bis(thiolate) chelate derivative of ethylenediamine, having square-planar Ni(II) coordination with an N_2S_2-ligand set, has a prominent absorption assigned to S_σ(thiolate) → Ni(II) LMCT at 37 000 cm^{-1} (270 nm) (Schugar, 1983). Similar 10 000–12 000-cm^{-1} red shifts are well documented for tetrahedral vs. tetragonal Cu(II) complexes (Schugar, 1983).

The resonance Raman spectrum of Ni(II)·LADH (406.7-nm excitation) is noteworthy in that the principal peaks are nearly coincident with those observed for the Cu(II) derivatives (Table I). This implies that the bonding and structural parameters of the tetrahedral site in the Cu(II) protein are preserved in Ni(II)·LADH. However, the resonance Raman spectrum of Ni(II)·azurin (Ferris et al., 1979) exhibits a significant shift of the principal azurin peaks to *lower* frequencies, suggesting that the copper and nickel forms of azurin are not as isostructural as in alcohol dehydrogenase. Although the resonance Raman and ^1H NMR spectra of Ni(II)·azurin have both been interpreted as arising from a tetrahedral metal site (Ferris et al., 1979; Blaszak et al., 1982), the tetrahedral assignment has been questioned on the basis of the failure to observe the $^3T_1 \rightarrow {}^3A_2$ absorption band in the near infrared spectra of either Ni(II)·azurin or Ni(II)·stellacyanin (Lum & Gray, 1981). It may be noted that the $S_\sigma \rightarrow$ Ni(II) charge-transfer bands at 440 nm for Ni(II)·azurin and at 410 nm for Ni(II)·stellacyanin, in particular, are close to the 407-nm absorbance of Ni(II)·LADH, which appears to have a tetrahedral site.

Conclusions

Crystallographic studies of native liver alcohol dehydrogenase have shown that the zinc site is tetrahedral and that this geometry is preserved in the presence of substrate analogues or inhibitors that coordinate directly to the zinc ion. The Raman studies presented here provide evidence that the tetrahedral character of the metal site is maintained in Cu(II)- and Ni(II)-substituted alcohol dehydrogenase and in the NADH and pyrazole complexes of the copper-containing enzyme. The fact that there are two spectral components that appear to be associated with Cu–S vibrations indicates that the two cysteinate ligands are structurally distinguishable. Moreover, the unusually high frequency of these vibrations implies that the Cu–S bond lengths in the dehydrogenase are likely to be as short as 2.1 Å, as has been observed for azurin and plastocyanin.

Copper-substituted alcohol dehydrogenase appears to be an excellent system for probing the properties of the blue copper proteins. Its electronic, EPR, and resonance Raman spectral properties more successfully match those of the type 1 proteins than do any of the presently available inorganic model complexes (Schugar, 1983). In the blue copper proteins, the structure of the protein is believed to be important in imposing a tetrahedral coordination geometry on the metal binding site and, thereby, facilitating the oxidation–reduction chemistry of the copper center (Williams, 1971; Gray & Solomon, 1981). Although the zinc in alcohol dehydrogenase is not involved in redox reactions, the maintenance of a tetrahedral geometry must also be critical in the function of that enzyme. It appears that the rather unfavorable tetrahedral geometries for Cu(II) and Ni(II) can be more readily attained by coordination to a specific metal binding site within a protein (e.g., alcohol dehydrogenase) than by complexation with low molecular weight ligands.

Registry No. LADH, 9031-72-5; NADH, 58-68-4; pyrazole, 288-13-1.

References

Andersson, I., Maret, W., Zeppezauer, M., Brown, R. D., III, & Koenig, S. H. (1981) *Biochemistry 20*, 3424-3432.
Blaszak, J., Ulrich, E. L., Markley, J. L., & McMillin, D. R. (1982) *Biochemistry 21*, 6253-6258.
Cedergren-Zeppezauer, E., Samama, J.-P., & Eklund, H. (1982) *Biochemistry 21*, 4895-4908.
Dietrich, H., Maret, W., Kozlowski, H., & Zeppezauer, M. (1981) *J. Inorg. Biochem. 14*, 297-311.
Dunn, M. F., Dietrich, H., MacGibbon, A. K. H., Koerber, S. C., & Zeppezauer, M. (1982) *Biochemistry 21*, 354-363.
Eklund, H., Nordström, B., Zeppezauer, E., Söderlund, G., Ohlsson, I., Boiwe, T., Söderberg, B.-O., Tapia, O., Brändén, C.-I., & Åkeson, Å. (1976) *J. Mol. Biol. 102*, 27-59.
Eklund, H., Samama, J.-P., Wallén, L., Brändén, C.-I., Åkeson, Å., & Jones, A. T. (1981) *J. Mol. Biol. 146*, 561-587.
Eklund, H., Samama, J.-P., & Wallén, L. (1982) *Biochemistry 21*, 4858-4866.
Fee, J. A. (1975) *Struct. Bonding (Berlin) 23*, 1-60.
Ferris, N. S., Woodruff, W. H., Tennent, D. L., & McMillin, D. R. (1979) *Biochem. Biophys. Res. Commun. 88*, 288-296.
Freeman, H. C. (1981) in *Coordination Chemistry* (Laurent, J. P., Ed.) Vol. 21, pp 29-51, Pergamon, Oxford.
Gray, H. B., & Solomon, E. I. (1981) *Met. Ions Biol. 3*, 1-39.
Loehr, T. M., Keyes, W. E., & Pincus, P. A. (1979) *Anal. Biochem. 96*, 456-463.
Lum, V., & Gray, H. B. (1981) *Isr. J. Chem. 21*, 23-25.
Maret, W., Dietrich, H., Ruf, H.-H., & Zeppezauer, M. (1980) *J. Inorg. Biochem. 12*, 241-252.
Maret, W., Zeppezauer, M., Desideri, A., Morpurgo, L., & Rotilio, G. (1981) *FEBS Lett. 136*, 72-74.
Maret, W., Zeppezauer, M., Desideri, A., Morpurgo, L., & Rotilio, G. (1983) *Biochim. Biophys. Acta* (in press).
Miskowski, V., Tang, S.-P. W., Spiro, T. G., Shapiro, E., & Moss, T. H. (1975) *Biochemistry 14*, 1244-1250.
Schneider, G., Eklund, H., Cedergren-Zeppezauer, E., & Zeppezauer, M. (1983) *Proc. Natl. Acad. Sci. U.S.A.* (in press).
Schugar, H. J. (1983) in *Copper Coordination Chemistry: Biochemical and Inorganic Perspectives* (Karlin, K. D., & Zubieta, J., Eds.) Adenine Press, New York.
Scott, R. A., Hahn, J. E., Doniach, S., Freeman, H. C., & Hodgson, K. O. (1982) *J. Am. Chem. Soc. 104*, 5364-5369.
Siiman, O., Young, N. M., & Carey, P. R. (1976) *J. Am. Chem. Soc. 98*, 744-748.
Sjöberg, B.-M., Loehr, T. M., & Sanders-Loehr, J. (1982) *Biochemistry 21*, 96-102.
Thamann, T. J., Frank, P., Willis, L. J., & Loehr, T. M. (1982) *Proc. Natl. Acad. Sci. U.S.A. 79*, 6396-6400.
Tullius, T. D., Frank, P., & Hodgson, K. O. (1978) *Proc. Natl. Acad. Sci. U.S.A. 75*, 4069-4073.
Williams, R. J. P. (1971) *Inorg. Chim. Acta, Rev. 5*, 137-155.

Association of Human γ Chain with Class II Transplantation Antigens during Intracellular Transport†

Lena Claesson* and Per A. Peterson

ABSTRACT: Cell surface expressed human and murine class II transplantation antigens are composed of two polypeptide chains called α and β. During intracellular transport an invariant chain, provisionally called γ, is associated with the class II antigen chains. Since γ chains leave the endoplasmic reticulum only when associated with α and β chains, we have studied the intracellular transport of the γ chain and its possible cell surface expression. Modifications of the carbohydrate moieties of the γ chain during intracellular transport were also examined. The γ chain appears to contain two Asn-linked carbohydrate moieties and maybe also one or more Ser/Thr-linked carbohydrates. At all times during the pulse–chase experiments core glycosylated γ chains resolved into two distinct spots on two-dimensional gel electrophoresis. The occurrence of core-glycosylated γ chains was expected since more γ chains than α and β chains exist in the endoplasmic reticulum. Terminally glycosylated, α, β, and γ chains emerged simultaneously supporting the idea that the three types of chains are brought to the Golgi complex bound to each other. However, terminal glycosylation is temporally related to the dissociation of the γ chain from the α and β chains. Since isolated plasma membranes contained molecules indistinguishable from γ chains, it is concluded that γ chains are transported together with class II antigens from the endoplasmic reticulum to the Golgi complex. After dissociation, class II antigens and some, if not all, γ chains seem to become independently integrated into the plasma membrane.

The major histocompatibility complex (MHC)[1] controls the expression of class II transplantation antigens [for a review, see Benacerraf (1981)]. These molecules are composed of two dissimilar, glycosylated chains, called α and β, which are expressed on the cell surface. In the mouse the I region encompasses two subloci, A and E, which each control the expression of a distinct type of class II antigen (Uhr et al., 1979). Likewise, the human MHC controls at least two types of class II antigens, i.e., HLA-DR antigens and DC antigens (Shackelford et al., 1981; Tosi et al., 1978). In addition, the

† From the Department of Cell Research, The Wallenberg Laboratory, University of Uppsala, S751 22 Uppsala, Sweden. *Received January 21, 1983.* This work was supported by grants from the Swedish Cancer Society and the Swedish Natural Science Council.

[1] Abbreviations: MHC, major histocompatibility complex; NaDodSO$_4$, sodium dodecyl sulfate; Endo H, endo-β-*N*-acetylglucosaminidase H; Tris, tris(hydroxymethyl)aminomethane; Mops, 3-(*N*-morpholino)-propanesulfonic acid.

0006-2960/83/0422-3206$01.50/0